Centromere-proximal crossovers disrupt proper homologous chromosome disjunction during meiosis

Sucharita Sen, Sneha Sarkar, Gopika Menon and Mridula Nambiar*

Department of Biology, Indian Institute of Science Education and Research, Pune 411008, Maharashtra, India

**To whom correspondence should be addressed*:

mridula@iiserpune.ac.in

Running title – Centromeric crossovers increase meiosis I segregation errors

Keywords – Meiotic recombination, Pericentric heterochromatin, Cohesins, Chromosomal mis-segregation, Aneuploidy

Abstract

Centromere-proximal crossovers are repressed during meiosis across all species. However, there is a strong correlation between aberrant centromeric crossovers (C-COs) and the occurrence of meiotic aneuploidy and disorders such as Down syndrome. Despite decades of work in understanding repression of C-COs, the molecular basis of how they cause chromosomal mis-segregation is unknown. Here, we show that increased C-COs result in improper separation of homologs leading to increased meiosis I errors and aneuploidy in *Schizosaccharomyces pombe*. C-COs cause nondisjunction events that cannot be explained by random segregation of homologs and additionally, may also disrupt mono-orientation of sister chromatids in meiosis I leading to their premature separation. We provide evidence that the protected population of cohesins at centromeres during meiosis I may interfere with timely resolution of C-COs causing homolog nondisjunction. These molecular insights will improve our understanding of infertility and aneuploidy-associated developmental disorders in humans.

Introduction

Meiosis involves segregation of homologous chromosomes during the first round of division while ensuring that the sister-chromatids stay close together. Disruptions in these mechanisms result in unequal distribution of chromosomes in the four gametes at the end of meiosis, which can severely affect their viability and lead to congenital developmental disorders such as Down syndrome characterized by presence of extra chromosomes [1]. Genetic recombination is critical during meiosis and allows shuffling of genes between the two parental chromosomes resulting in enhanced genetic diversity in the progeny. Recombination is mediated by homology-directed DNA repair in response to programmed double-strand breaks (DSBs) generated by the evolutionarily conserved Spo11, in complex with other associated proteins [2]. The recombination intermediates can be resolved to either result in a crossover or non-crossover event, the former resulting in a matured chiasma that can be seen as physical connections between the homologs in meiosis I (MI) [3].

Apart from generating diversity, crossovers contribute towards facilitating proper separation of homologs during MI along with cohesin complexes that hold the sister-chromatids together after replication [4]. Systematic removal of these cohesin complexes helps regulate meiotic chromosome segregation – the cohesins in the arms are removed at anaphase I, but those at the pericentric regions are protected till meiosis II (MII) by Shugoshin (Sgo1), to facilitate proper segregation, similar to mitosis [5,6]. The distribution of crossovers is not uniform across the genome and are deleterious, if they occur within or near centromeres [7]. Studies in many diverse species done till date demonstrate the near absence of crossovers at the centromeres as well as the pericentric regions and a distance-dependent reduced frequency in the flanking euchromatin regions, better known as the centromere effect [8].

Our previous study in *Schizosaccharomyces pombe*, demonstrated the critical role of the centromere-specific cohesin complex containing the meiotic kleisin subunit Rec8 and the HEAT repeat associated with kleisin (HAWK) subunit Psc3, in mediating the repression of meiotic crossovers at the pericentric regions flanking the centromeres [9]. Active exclusion of the pro-recombinogenic cohesin complex consisting of Rec8 and Rec11 (meiotic paralog of Psc3) from the centromeres, prevents activation of the DSB-inducing Rec12 (Spo11 ortholog) complex from initiating DSB formation and further homology-directed repair. Forceful targeting of the Rec12 complex-activating protein Rec10 in an otherwise wild type genetic background or targeting the Rec8-Rec11 cohesin complex to the pericentric regions in the absence of Psc3, dramatically increased DSBs and consequently centromeric crossovers (C-COs) [9]. It was also suggested that the heterochromatin protein 1 (HP1) ortholog Swi6 may contribute in

establishing a cohesin loading bias via its interaction with the Psc3 cohesin subunit. Hence, this repression of recombination is extremely well-regulated and its absence has been positively correlated to the occurrence of trisomies and aneuploid foetuses resulting in l miscarriages in humans [10].

Increased chromosomal mis-segregation events that are seen in older oocytes from many species such as flies, mice and humans can be mainly attributed to improper recombination as well as the absence of cohesin turnover that results in weakened centromeric and sister-chromatid cohesion [11]. The former includes both absence of chromosomal crossover events or aberrant centromere-proximal crossovers. Multiple linkage studies in human trisomy cases such as Down syndrome have found a strong correlation between centromere-proximal crossovers and the occurrence of non-disjunction (NDJ) events. A study in budding yeast *Saccharomyces cerevisiae* showed elevated premature separation of sister chromatids (PSSC) in MI in presence of C-COs [12,13]. In contrast, spontaneous X chromosome NDJs in *Drosophila* as well as human trisomy 21 cases showed that centromere-proximal exchanges were associated primarily with MII NDJ [14–16]. However, despite being an age-old problem, the mechanistic basis of how C-COs result in chromosomal mis-segregation is not completely understood in any species. This question is particularly of interest as crossovers occur amply in the chromosomal arms to facilitate genetic diversity as well as promote faithful MI homolog segregation, but cause mis-segregation when present at the centromeres.

Here, we employed *S. pombe* with activated C-COs to determine the source of segregation defects during meiosis. We find that the segregation errors arise primarily due to non-disjunction of the homologs at MI and also additionally via disruption in mono-orientation leading to premature separation of sister chromatids. The origin of these MI errors cannot be attributed to reduced centromeric cohesins, disrupted pericentric heterochromatin or decreased levels of arm crossovers. We provide evidence for a critical role of the residual protected pericentric cohesin population at the end of MI, to contribute towards non-disjunction of homologs in the presence of C-COs, which is in contrast to its fundamental role in promoting accurate segregation in MII. This study also provides molecular insights to understand how perturbing the spatially regulated crossover control at the centromeres and chromosomal arms can lead to similar erroneous phenotypes but are explained by distinct mechanisms. Since, *S. pombe* pericentric and centromeric regions are excellent experimental substitutes for mammalian centromeres, our study will be relevant in better understanding the defects arising during oogenesis and its association with genetic disorders.

Results

Different types of mis-segregation defects can be captured based on the source of the erroneous step during meiosis

In order to quantifiably observe and categorise chromosome segregation defects during the two stages of meiosis, we employed the previously developed fluorescence-based tetrad assay in *S. pombe* [17]. The fluorophore gene is inserted close to *cen1* (centromere of chromosome 1) under the effect of a spore autonomous promoter such that it is only expressed upon sporulation. Upon completion of meiosis, the four spores within the ascus are arranged in an ordered manner, such that spores on each half of the ascus are formed from the same MI nucleus (Fig. 1A, image 1). In a wild-type meiosis with normal segregation, the profile is expected to be such that the set of first two and last two spores would be like-coloured. Any deviation from such a visual profile would mean deviation from a normal segregation pattern. We worked out additional possible categories of segregation error profiles that weren't discussed previously, and split the errors originating in MI into those that can arise due to non-disjunction (NDJ) of homologs, wherein the homologs fail to separate in MI and premature separation of sister chromatids (PSSC), wherein sister chromatids separate in MI

itself, towards opposite poles (Fig. 1A, images 6-16). MII errors during segregation primarily arise due to MII NDJ, wherein sister chromatids fail to separate (Fig. 1A, images 17-19). Another possible type of aberrant segregation can occur via reverse segregation (RS), where MI is equational (sister chromatids segregate) and meiosis II is reductional (homologs separate). This is different from a combination of two individual PSSC events as the frequency of occurrence of equational division due to reverse segregation is nearly 100 times higher than the expected frequency of a combination of two PSSC events as observed in human oocytes [18]. Alternatively, in an event of a crossover between the centromere and the fluorophore, the segregation profile will look identical to the reverse segregation profile (alternate colour pattern in each half of the ascus), upon normal segregation thereafter in MI and MII (Fig. 1A, images 2,3). In order to distinguish between the two, we additionally looked at the centromeric recombination frequency in such genotypes via genetic recombination assays. Since this assay cannot distinguish between RS and C-CO associated phenotypes by itself, we have named this category as an RS/C-CO phenotype. Additionally, tetrads that undergo a C-CO followed by MI missegregation, would still show the same phenotype as normal MI NDJ or PSSC events. In contrast, if a C-CO is followed by normal MI segregation but erroneous MII segregation, a distinct profile will be observed that cannot result from any other source (Fig. 1A, images 4,5).

Increased centromere-proximal crossovers are associated with elevated errors at meiosis I

In *S. pombe*, active exclusion of a functional Rec8-Rec11 cohesin complex at the pericentric heterochromatin prevents the pro-recombinogenic cascade of proteins including the linear element (LinE) proteins such as Rec10 to be recruited at the centromeres [9,19]. We previously showed that forced recruitment of Rec10 to the pericentric heterochromatin by fusing it with the H3K9Me-binding chromodomain (CD) dramatically increases meiotic recombination frequency across fission yeast centromeres *cen1* and *cen3* [9]. However, this concomitantly led to a significant decrease in recombination frequencies across chromosomal arm intervals, due to redistribution of a significant percentage of Rec10 population to the centromeric and other heterochromatin regions. Since reduced arm COs also compromise chromosomal segregation fidelity, we wanted to establish a genetic background where C-COs may be the only source of segregation errors. Hence, we first checked whether over-expressing Rec10 ectopically in a *rec10*Δ genetic background could rescue the segregation defects and confirmed the expression via immunoblotting (Suppl. Fig. 1A). We noted that the asci formed in the *rec10*Δ background, were visually severely defective, with abnormal shapes and number of spores (Suppl. Fig. 1B). Hence, to determine the segregation defects using the tetrad assay, we only evaluated asci with four spores. The error profiles in the *rec10*Δ strains prominently showed MI errors, wherein NDJ events were 39.6% while the PSSC events were 16.8% (Fig. 1B). However, upon ectopic expression of Rec10 in the *rec10*Δ background, the total segregation errors came down by almost 90%, indicating that the ectopically expressed Rec10 was able to rescue the reduced arm recombination-associated segregation defects in *rec10*Δ background.

In order to study the deleterious effects of increased C-COs on meiotic chromosome segregation, the assay was performed in the *rec10-CD rec10ee* genotype with confirmed ectopic expression (ee) of Rec10 (Suppl. Fig. 1C). *rec10-CD* alone showed only 41.1% tetrads with normal segregation, whereas most of the errors were contributed by abnormal MI segregation (33.3%), followed by 17.7% MII errors (Suppl. Fig. 1D). We also observed a significant fraction of tetrads (8.1%) showing C-COs phenotype confirming the activation of meiotic recombination events at the otherwise repressed centromeres (Suppl. Fig. 1D). In contrast, when Rec10 was ectopically overexpressed in the presence of *rec10-CD*, the percentage of normal segregation increased to 72.2%, without significantly affecting frequency of C-COs (7.3%) (Fig. 1C and Suppl. Fig. 1D). Importantly, the MI errors were still significantly high in the presence of *rec10-CD rec10ee* (13.8%), especially when compared to a

rec10(mut)-CD rec10ee (6.8%), where the C-COs were nearly abolished and MII errors largely remained the same (Fig. 1C). The ectopic Rec10 expression was able to dramatically reduce all the error classes even in presence of *rec10(mut)-CD,* suggesting that the lowered arm recombination-associated defects were rescued similar to *rec10*Δ (Suppl. Fig. 1D). Moreover, we find that most of the errors observed in presence of *rec10-cd* were lost upon using a *rec10-cd(mut)* allele that has a W104A mutation in the CD domain, making it unable to bind to H3K9me histones at the heterochromatin [20] (Fig. 1C). Hence, we can conclude that the elevated frequency of C-COs is strongly associated with increased meiosis I errors. Interestingly, within this class, we observed a bias towards MI NDJ as compared to MI PSSC events (Fig. 1D and Suppl. Fig. 1E). Out of the total tetrads showing MI errors, 54.4% were contributed by MI NDJ in *rec10-CD rec10ee*, while MI PSSC occurred in 45.6% tetrads (Fig. 1D). Overall, these data show that C-COs in *S. pombe* disrupt accurate disjunction of homologous chromosomes during meiosis I.

Absence of chromosomal arm crossovers also exhibits meiosis I defects similar to C-COs

Since crossovers in the chromosomal arm regions are known to aid in proper homolog disjunction at meiosis I, our results suggest that centromeric crossovers elevate homolog non-disjunction appear counterintuitive. Hence, we wanted to determine the type of MI errors in mutants defective at different points of DSB initiation. Phosphorylation of the meiotic cohesin subunit Rec11, helps recruit Rec10, which further activates the Rec12 complex to initiate DSB formation in *S. pombe*. We used *rec11*Δ*,* a phosphodeficient mutant *rec11(5A)*, and *rec12*Δ to study the errors in segregation and compared to *rec10*Δ as well (Fig. 2A). Both *rec11*Δ and *rec11(5A)* showed a higher incidence of MI errors (40.9% and 18.3%, respectively), wherein approximately 29% and 13% were contributed by MI NDJ in *rec11*Δ and *rec11(5A)*, while MI PSSC occurred at 11.9% and 5.3%, respectively (Fig. 2A, B). *rec11(5A)* showed overall lesser MI errors as compared to *rec11*Δ possibly due to intact arm cohesion-associated functions (Fig. 2A). In addition, the *rec11(5A)* mutant still retained significant recombination frequency at the *ade6-arg1* interval compared to *rec11*Δ that had completely abolished recombination, suggesting possibly additional phosphorylatable sites on Rec11 apart from the 5 modified sites (Fig. 2C). Compared to *rec10*Δ*,* the *rec11* mutants had lower MI errors, but similar MII errors (Fig. 2A-C). Similarly, *rec12*Δ primarily showed increased MI errors, with 43.9% NDJ events and 11.7% PSSC and interestingly a significantly high population of MII errors (19.8%) compared to the wild type (Fig. 2A, B). The increased MII errors may be due to a previously reported non-topoisomerase catalytic activity of Rec12, which is required for proper segregation fidelity of sister-chromatids in meiosis II [21]. Since both *rec10*Δ and *rec12*Δ are completely recombination deficient, the non-disjunction of homologs in meiosis I may not reflect the classical inability of the chromosomes to separate and segregate into the same nucleus. Loss of physical connections between homologs would result in random segregation of the chromosomes with both the sister chromatids still together, unlike PSSC. This is also supported by the nearly 50% MI errors seen in *rec10*Δ and *rec12*Δ that reflect random homolog segregation. Therefore, these are better classified as MI "NDJ-like" events in such recombination-deficient mutants.

Loss of centromeric cohesion does not lead to increase in meiosis I errors

The pericentric cohesin complex is different from that of the arms in having Psc3 as the HAWK subunit as compared to Rec11, while the trimeric ring Psm1-Psm3-Rec8 stays the same [19]. This complex is also essential for maintaining chromosomal segregation fidelity in MI, since the centromeric cohesion needs to be preserved at anaphase I to keep sister chromatids attached to each other and favor disjunction of homologs. Weakened centromeric cohesion, which is elevated in aged mammalian oocytes, increases rates of meiotic aneuploidy [22]. We wondered if the elevated MI errors in case of increased C-COs could be due to loss of pericentric cohesion triggered during the process of Holliday Junction formation or resolution of recombination intermediates upon Rec12-induced DSBs. If so, the errors generated in

genotypes that are unable to establish, maintain or preserve pericentric cohesion, should mimic those generated during C-COs formation (Fig. 3A).

First, we tested meiotic segregation fidelity in *psc3*Δ cells, which can survive if the meiotic cohesins Rec8 and Rec11 are ectopically expressed in vegetative cells [19]. Upon completion of meiosis in the absence of Psc3, a dramatic 74.2% tetrads showed MII errors due to random sister-chromatid separation arising from the absence of the critical centromeric cohesion (Fig. 3B). There were only 13.4% normal tetrads and merely 10.8% tetrads showing MI errors. As expected, there were no significant C-COs seen, supporting genetic recombination data determined previously [9] (Fig. 3B). This overwhelming skew toward MII errors points towards the roles of Psc3, as part of the centromeric cohesin complex, mainly during segregation of sister-chromatids. The protection of this centromeric cohesin population is facilitated by the Sgo1-PP2A complex that binds to and prevents cleavage of the Rec8-Psc3 complex by inhibiting its phosphorylation by the CK1 kinase [23] (Fig. 3A). Hence, disruption of this protection should show similar segregation defects. As expected, in *sgo1*Δ, 85.8% tetrads showed MII errors, with close to no normal segregation, which interestingly is a much more severe phenotype than *psc3*Δ, reiterating that failure to preserve the centromeric cohesion caused mainly meiosis II errors (Fig. 3B). *sgo1*Δ has normal chromosomal arm recombination frequency across the measured *cen3-ade6* genetic interval, compared to wild type and no increase in recombination across *cen3* (Fig. 3C and D). Deletion of the catalytic subunit of the PP2A complex, *ppa2*Δ, did not phenocopy *sgo1*Δ and was mostly indistinguishable from wild type, except for a relatively lower but significant increase in MII errors (11.6%) as compared to *psc3*Δ and *sgo1*Δ (Fig. 3B). There were no dramatic differences in the frequency of genetic recombination across the measured intervals in arms and *cen3* in *ppa2*Δ, compared to wild type (Fig. 3C and D). Overall, disruptions in centromeric cohesion dramatically elevated errors in sister-chromatid segregation in MII, much more than affecting homolog disjunction in MI. In all these cases, since the chromosomal arm cohesion by Rec8-Rec11 complex is retained and the crossover formation in the arm is unhindered, it could be expected that the homolog disjunction will not be affected.

Disruption of pericentric heterochromatin elevates meiosis II errors unlike centromere-proximal crossovers

Next, we checked whether perturbation in the pericentric heterochromatin functions due to C-COs may be contributing to the increased MI errors. Heterochromatin protein HP1 orthologs, Swi6 and Chp2, recognize and bind the histone H3K9me epigenetic marks and help in heterochromatin assembly and silencing functions (Fig. 3A). Additionally, Swi6 promotes deposition of the Rec8-Psc3 cohesin complex at the pericentric heterochromatin to facilitate sister-chromatid cohesion [24]. On the other hand, Chp2 promotes histone deacetylation during heterochromatin assembly by recruiting the SHREC complex [25]. We tested whether disruption of heterochromatin activity in the absence of either Swi6 or Chp2, affected segregation fidelity and observed an increased frequency of MII errors upon *swi6*Δ (47.2%), which was much less severe than both *psc3*Δ and *sgo1*Δ (Fig. 3B). Both C-CO and MI errors were not different among these three genotypes. Interestingly, in *chp2*Δ the effects were unlike its paralog and nearly wild type, suggesting that disrupting heterochromatin gene silencing functions do not play any role in maintaining chromosomal segregation fidelity (Fig. 3B). In contrast, affecting heterochromatin's role in centromeric cohesin deposition severely compromises segregation fidelity, thereby providing evidence for another non-overlapping function of the HP1 paralogs Swi6 and Chp2. Hence, we can infer that loss of functional heterochromatin cannot explain the elevated MI errors due to C-COs, since such mutants also show predominantly MII errors, which is in agreement with the previously described low levels of Rec8-Psc3 cohesins and consequently centromeric cohesion in a *swi6*Δ genotype [24].

Residual pericentric cohesins at MI contribute towards homolog non-disjunction by centromeric-crossovers

It is interesting that increased meiosis I errors can be caused by both “derepressed” recombination events at the centromeres and “repressed” recombination at the chromosomal arms. How can gain in crossovers on one part of the chromosome result in a homolog non-disjunction phenotype similar to the loss of crossovers in another? One of the major differences between the two regions is the cohesin dynamics during late prophase I. The centromeric cohesin population is protected till sister-chromatid separation at MII, while the arm cohesins are proteolytically cleaved [26]. Removal of cohesins distal to the chiasma is necessary to facilitate separation of the homologs that underwent recombination [4,27]. Could the persisting centromeric cohesins promote the observed MI NDJ events, when C-COs occur that are otherwise repressed? In the absence of the centromere-specific cohesin subunit Psc3, there is a high frequency of MII errors and no activation of C-COs, as established above (Fig. 3B). In this background, we planned to activate C-COs by targeting Rec8-Rec11 complex via chromodomain fusions, which previously has been shown to derepress pericentric recombination [9] (Suppl. Fig. 2A). We compared this with a *rec11(5A)-CD* mutant that is recombination-deficient at the chromosomal arms. An ectopic copy of the wild type Rec11 (*rec11ee*) was expressed in these genotypes to maintain a robust frequency of chromosomal arm crossovers and rule out any MI segregation defects due to reduced arm recombination. We confirmed the rescue of MI defects arising in presence of *rec11*Δ or *rec11(5A),* as seen above, via the ectopic expression of the *rec11* allele (Suppl. Fig. 2B). Interestingly, neither targeting Rec8-Rec11 complex to pericentric regions via CD nor presence of *rec11ee* were able to rescue the severe MII defects in *psc3*Δ (Suppl. Fig. 2C). However, we also didn’t observe any significant differences in the C-CO or MI errors in *psc3*Δ *rec8-CD rec11-CD rec11ee* compared to *psc3*Δ *rec8ee rec11ee* (Suppl. Fig. 2C). We suspect that due to the high levels of MII errors and consequences of loss of centromeric Psc3 on sister-chromatid cohesion, we might be unable to detect the majority of the C-CO events and consequent MI errors. Moreover, the phosphodeficient mutant *rec11(5A)-CD* in this genotypic background, didn’t reduce the 8-11% of MI errors seen in the *psc3*Δ *rec8-CD rec11-CD rec11ee* strain, probably due to the presence of an ectopic copy of wild type Rec11 that may also access the centromere along with Rec8-CD (Suppl. Fig. 2C). One striking observation of the MI errors in the absence of Psc3, was a conspicuous change in the distribution of the fraction of MI error subtypes (Fig. 4A and Suppl. Fig. 3B). There was a dramatic increase in MI PSSC events as compared to MI NDJ events in *psc3*Δ genotypes, which was in stark contrast to that observed in *psc3+ rec10-cd* strains as shown above (Compare Fig. 4A and Fig. 1D).

This clearly suggested that lowering the pericentric cohesin population might aid in reducing the MI NDJ events due to unresolved centromeric crossovers between homologs. In order to further strengthen this observation, we employed *swi6*Δ, as a way to reduce the cohesins in the vicinity of the C-COs generated by *rec10-CD rec10ee,* since overall, the frequency of MI and MII errors was lesser in *swi6*Δ compared to *psc3*Δ [24] (Fig. 3B). As expected, we observed a significant increase in the total MI errors due to *rec10-CD* in *swi6*Δ as compared to *swi6*Δ alone, which could also be due to more recruitment of Rec10-CD to the H3K9me heterochromatin, in absence of the competing Swi6 (Fig. 4B). We also observed a significant increase in the total MI errors in the presence of *swi6*Δ as compared to Rec10-CD alone and within this, MI PSSC events increased significantly and not MI NDJs (Fig. 4B and Suppl. Fig. 3A). However, if we compare the individual fractions of the subtypes among the total MI errors, we continued to observe a significantly marked reduction in the MI nondisjunction events and a concomitant increase in levels of PSSC phenotype (Fig. 4C and Suppl. Fig. 3B). This suggests that presence of the protected population of pericentric cohesins during anaphase I, may hinder the timely resolution of the C-COs, resulting in the nondisjunction of the homologs, which gets lowered upon lowering cohesion (Suppl. Fig. 3B). Additionally, our data also indicates that C-COs may also interfere with the appropriate monopolar attachment of the sister chromatids, resulting in premature separation of atleast one pair of sister chromatids, which gets exacerbated upon reducing the pericentric cohesin levels during meiosis (Suppl. Fig. 3B).

Discussion

Repression of recombination across the centromeres is a conserved phenomenon across several species. However, the mechanisms by which this repression is mediated is found to vary among species, owing to differences in complexities in centromere organisation and the associated factors. Notably, stark differences in the repression mechanisms exist between the two highly diverged yeast species, *S. cerevisiae* and *S. pombe.* At budding yeast point centromeres, this repression is mediated mainly by the inner-kinetochore Ctf19 complex that helps deposit cohesins in the flanking pericentric regions and consequently favor inter-sister DSB repair over the expected inter-homolog repair, thereby preventing formation of crossovers [28,29]. In contrast, at fission yeast centromeres, crossover repression is mediated by preventing loading of a subtype of cohesin complex that promotes initiation of Spo11-mediated DSB formation, by the heterochromatin protein Swi6 [9,29]. Interestingly, not a lot is known about how centromeric crossovers hamper fidelity during meiotic chromosome segregation, especially given that chromosomal arm crossovers are vital for maintaining proper segregation. In *S. cerevisiae*, elevated incidence of premature separation of sister chromatids (PSSC) was reported in mutants derepressed for centromeric crossovers that eventually also contributed to increased MII errors [12]. Data from spontaneous X chromosome nondisjunctions in *Drosophila* and human trisomy 21 cases hint at the C-COs probably being associated with increased MII nondisjunctions [14,15]. More recent studies on human oocytes show specific segregation error types to have age dependencies [30]. For example, nondisjunction events due to aberrant recombination outcomes were found to be predominant in younger women, whereas pericentric cohesion loss affected women with increasing age. In order to mechanistically understand the consequences of C-COs on meiotic segregation in *S. pombe,* we used a previously established system to induce meiotic DSBs at the pericentric heterochromatin by targeting Rec10, a linear element protein involved in activation of the DSB forming protein Rec12, followed by analysis of the type of meiotic division errors generated. In addition, our data provide an in-depth coverage of the segregation defects caused by perturbations in centromeric cohesion, meiotic recombination and heterochromatin establishment, in either or both the stages of meiotic division, for all the four products of one round of meiosis. This would be challenging to establish in humans, due to asymmetric division during oogenesis.

The centromere is different from the euchromatic chromosome arm regions in (i) having a constitutive pericentric heterochromatin (ii) being the center for kinetochore assembly and (iii) intact sister-chromatid cohesion at the end of meiosis I, as opposed to arm regions where cohesins are cleaved off at anaphase I. In order to decipher the mechanistic basis of why C-COs are deleterious, whereas arm COs are not, we studied cells exhibiting increased C-COs in Rec10-CD expressing cells. We observed predominantly MI errors with a bias towards NDJ events i.e. both the homologs migrating to the same MI nucleus over PSSC, where separation of one of the sister chromatids occurs at MI itself (Fig. 1A and 1C). Since, here the pericentric cohesins (Rec8-Psc3 complex) and heterochromatin are intact, this may imply that the recombination intermediates fail to resolve, leading to a failure to separate homologs. Another explanation for both homologs to segregate into the same nucleus at MI may be by random chance. Cells with defective arm recombination show errors in segregation and we similarly observed increased frequency of tetrads displaying MI NDJ-like events in *rec12*Δ and *rec10*Δ (Fig. 2A). We also observed a similar trend in *rec11*Δ and the phosphorylation deficient mutant *rec11(5A),* which can't recruit Rec10 to initiate recombination, but maintains its cohesion-associated function. However, the *rec11* mutants showed lower MI errors compared to *rec12*Δ and *rec10*Δ*,* probably due to some basal Rec11-independent recruitment of Rec10 [31]. We are reclassifying such MI errors arising due to abolished recombination as "NDJ-like" events as

they represent random homolog segregation and as expected have a frequency of ~50% (Fig. 2A and 2B). This represents a unique class of defects as gain in crossovers at the centromeric regions results in the same phenotype as the loss of crossovers in the chromosomal arms. Even though the resulting erroneous tetrads may look the same, we propose that their origins can be explained by distinct mechanisms. In diploids, where homologous chromosome pairs are present, the occurrence of recombination events in the chromosomal arm regions is crucial for the fidelity of monopolar attachment of sister chromatids in MI [32]. In the absence of DSB initiation such as in *rec12*Δ or *rec10*Δ, and thereby loss of physical contact via crossovers between homologs, monopolar attachment would be disrupted, thereby elevating NDJ-like events due to random segregation. In contrast, the MI NDJ phenotype observed in case of a centromeric crossover might be a direct readout for an actual failure to resolve the chiasma, leading to "entangling" of the homologs, causing MI nondisjunction events. Therefore, we hypothesized that the cohesin and heterochromatin rich pericentric regions that contribute to protection of the centromeric cohesin population during anaphase I, may prevent the resolution of crossovers, leading to MI NDJ.

Removal of factors necessary for sister-chromatid cohesion at the centromeres such as Psc3 and Swi6 did not show a similar nondisjunction phenotype at MI but did so at MII (Fig. 3B). This increase in MII errors is also mimicked by centromeric cohesin protectors at anaphase I such as SgoI and PP2A complex, with Sgo1 loss resulting in a high percentage of MII errors, with close to no normal segregation. Interestingly, deletion of the catalytic subunit of the PP2A complex, Ppa2, showed only a minor but significant increase in MII errors. This is in agreement with a previous report that deletion of the Par1-B subunit of the PP2A complex, and not the catalytic subunit Ppa2, showed segregation errors comparable to *sgo1*Δ [33]. This may also suggest contribution of other phosphatases apart from PP2A that could preserve Rec8 from cleavage in its absence. Thus, we infer that loss of pericentric cohesion, either by failure of establishment or preservation of the cohesin population, cannot explain the increase in MI NDJ error type, observed in the C-CO proficient meiotic cells. However, removal of cohesins distal to the site of crossovers is important for the resolution of the chiasma [34]. Uncleaved cohesins in the chromosomal arms as observed in the presence of non-phosphorylatable Rec8, fail to get removed from the chromosomes at anaphase I, and predisposes the homologs to undergo increased nondisjunction [35]. Deleting cohesin Rec11 in the same genotype, and thereby reducing overall arm cohesin, drastically alleviates this MI NDJ phenotype, but consequently contributes to MII errors. Hence, persistence of pericentric cohesion due to protection of the cohesin complexes from separase-mediated cleavage as happens in the chromosomal arms during anaphase I, may result in entangled homologs when induced for C-COs resulting in elevated MI NDJ. A previous report showing an MII oocyte having two homologous chromosomes connected at the centromeres with centromeric REC8 and SGO1 encompassing both sets of sister kinetochores, suggests that cytologically such a scenario where the homologs remain stuck to each other is possible that can contribute to gametic aneuploidy [34]. In order to test this hypothesis, we would need to remove pericentric cohesins Rec8-Psc3 at anaphase I; however, *psc3*Δ is lethal and requires ectopic expression of Rec8 and Rec11 for survival. Using *rec8*Δ or loss of function Rec8 mutants is not feasible, since Rec8 regulates both centromeric and arm cohesion levels in meiosis, and more importantly, Rec8 is a key centromeric player in maintaining mono-orientation of sister kinetochores during MI, failure of which, leads to equational division in MII. The readout for such disrupted monopolar attachment in this assay, is a large increase in the C-CO/RS profile (unpublished data from the lab). Additionally, the presence of constitutive heterochromatin at the pericentric regions could also contribute to the increased C-CO associated MI NDJ phenotype. We show that the increase in MII errors in case of *swi6*Δ correlates with its function in establishing physiological levels of Rec8-Psc3 cohesion at the pericentric regions (Fig. 3B).

This is independent of its heterochromatin and gene silencing function, as removal of the other HP1 paralog Chp2, results in minimal errors and near wild type chromosome segregation compared to *swi6*Δ. Hence, loss of centromeric cohesion cannot justify the MI NDJ error phenotype when C-COs are present, whereas persistent cohesion at the pericentric regions during MI may be one of the key factors in mediating this increased MI nondisjunction.

In order to directly test this hypothesis, we attempted to test the effect of removing centromeric cohesion while concomitantly elevating C-COs by targeting the arm cohesin complex containing Rec8-Rec11 to the pericentric regions via chromodomain fusions in *psc3*Δ that was shown before to increase C-COs [9]. We noticed a high frequency of MII errors similar to *psc3*Δ, even though C-COs were elevated, due to the dominant effect of Psc3 removal (Suppl. Fig. 2C). Using the phosphorylation deficient Rec11 mutant in the same background, did not seem to significantly alter any defects, due to presence of a wild type ectopically expressed copy of Rec11, which is indispensable for rescuing *psc3*Δ. Surprisingly, the C-CO and MI error profiles were similar for *psc3*Δ independent of targeted Rec8-Rec11 complex, in contrast to the increased recombinant frequencies seen using genetic assays, only when Rec8-Rec11 was targeted to the pericentric regions in *psc3*Δ background, in our previous study [9]. This also highlights the inability of the Rec8-Rec11 complex to compensate for the loss of Psc3 and thereby completely rescue MII errors, despite being targeted directly to the centromeres. This may possibly indicate the inability of the Rec8-Rec11 complex to be protected from separase cleavage during anaphase I at the centromeres by Shugoshin. The striking observation, however, was the dramatic dip in the frequency of MI NDJ among the total MI errors and its redistribution into the MI PSSC category (Fig. 4A). This supports the idea that loss of centromeric cohesion may facilitate chiasma resolution at the pericentric regions and aid in the separation of homologs. The increased PSSC could potentially be a reflection of the disrupted sister chromatid cohesion and possibly monopolar attachment due to altered cohesin population at the centromeres. We further confirmed these observations in a *rec10-CD swi6*Δ background, where the levels of pericentric cohesion would be reduced, without any changes to the arm COs or distribution of the native cohesin population. We found that similar to the *psc3*Δ background, there was a significant redistribution of the subtypes within the total MI errors (Fig. 4B). When we compare the effects of cohesin reduction either directly or via removal of Swi6, we observe a significant drop in NDJ and concomitant increase in the PSSC events among the total MI errors. The C-CO frequency in *swi6*Δ cells didn't change in the presence of Rec10-CD, probably due to improved resolution of the crossovers, leading to PSSC, which was significantly increased in this genotype (Fig. 4B and Suppl. Fig. 3A). We strongly suspect that homolog nondisjunction appears to be a dominant fraction of errors, since it might overshadow any potential loss in monopolar attachment that may occur in presence of C-COs, due to both homologs getting entangled and moving towards the same pole. However, in a pericentric environment with lowered cohesin and improved C-CO resolution, the errors in monopolar attachment may be more pronounced, resulting in the marked increase in PSSC events. These cannot be explained entirely by loss of pericentric cohesin, as *psc3*Δ or *swi6*Δ alone do not show the same phenotype. It is plausible that intact arm cohesion conferred by the Rec8-Rec11 complex along with mono-orientation factors such as Moa1 are sufficient to impart correct MI segregation and manifest the errors only in MII during sister chromatid separation, similar to *sgo1*Δ mutants. This is supported by observations in a recent study, wherein presence of single chromatids was found to be rare in MI human oocytes obtained irrespective of the donor age, indicating that maintenance of sister chromatid cohesion relies on centromeric cohesion only after removal of chromosomal arm cohesins at anaphase I [36].

Overall, our study provides sufficient evidence to support the following model for the long known, but poorly understood reason for how the centromere-proximal crossovers cause disruption of proper chromosome segregation, despite arm crossovers being critical for the same (Fig. 5). C-COs due to their position at the centromeres are unable to get resolved in the absence of cohesin removal during anaphase I, resulting in entanglement of the recombining homologs along with the paired sister-chromatids and thereby segregating into the same nucleus upon completion of MI. This gives rise to the classical "nondisjunction" phenotype of the homologs (Fig. 5). Additionally, we suspect that C-COs may also interfere with the proper monopolar attachment of either one or both the pairs of sister chromatids. When it occurs for one pair of sister chromatids, it results in a PSSC event. However, if it occurs on both it would lead to reverse segregation phenotype, i.e. equational division of both homologs and since this involves one completed C-CO event, the tetrad can be categorized both as C-CO or RS event. In contrast, lack of crossovers in the chromosomal arms would lead to random separation of either homolog into the same nuclei, resulting in "NDJ-like" phenotype. This pattern of increased MI NDJ in cohesion intact centromeres has also been reported in human oocytes from younger females, which progressively shifts to a PSSC defect with increasing age and consequent weakening of centromeric cohesion [30]. Another point to note is that MI NDJ events nearly always lead to all aneuploid spores upon one round of meiosis; however, MI PSSC, in most cases, would atleast have 50% euploid spores. Hence, crossovers at the centromeres if timely resolved or upon removal of cohesin from their vicinity (similar to that in the chromosomal arms during anaphase I), may be relatively less deleterious, and can improve the chances of obtaining euploid spores for preventing developmental disorders arising due to trisomy in humans.

Methods

Strains and genetic methods

The genotypes of the *S. pombe* strains generated and used in this study are described in Supplementary Table 1. Strains were generated by meiotic crosses followed by random spore analysis, as previously described [37]. Strains with temperature-sensitive alleles were grown at 25ºC, while the rest were cultured at 30ºC. Oligonucleotides and plasmids are described in Supplementary Tables 2 and 3, respectively. Colony PCRs were performed for genotyping.

S. pombe transformation

Transformations were done using the lithium acetate method, as described previously [38]. Briefly, log phase cells at OD_{600} of 0.3-0.4 (~1X10^7 cells) were cultured in appropriate media and after washing, resuspended in TE/LiOAc buffer (0.1 M of LiOAc in TE buffer) and incubated at 30ºC for 30 min. The cells were then pelleted and resuspended in TE/LiOAc buffer containing 40% PEG4000 and 50µg boiled salmon sperm DNA (Invitrogen, 15632011), with or without ~1 µg plasmid DNA and incubated at 30ºC for 30 min. Post incubation, the cells were given a heat shock at 42ºC for 20 min after adding DMSO. The cells were collected and allowed to recover in the appropriate media at 30ºC for 20-22 hours, followed by selection on appropriate media. For expression of Rec10, plasmid ME46 was transformed in MP1063, MP1064, MP208, MP238, MP109, MP244, MP183, MP1011, thereby generating MP1065, MP1066, MP1012, MP1013, MP1014, MP1015, MP1016 and MP1017, respectively (Suppl. Table 1). The transformants were confirmed by colony PCRs to either detect the plasmid or the correct genomic integrations.

Cloning of *rec10* for ectopic overexpression

Using *S. pombe* genomic DNA as template, a DNA construct containing *rec10* gene flanked by BamHI (forward primer*)* and SmaI (reverse primer) sites was amplified using primers MO323 and MO324 (Suppl. Table 2). Plasmid ME40 and the DNA construct were digested with BamHI and SmaI and further treated with alkaline phosphatase (Takara, 2250A) to prevent religation of the vector. The digested products were ligated to generate plasmid ME46 containing N-terminal *3X-myc* tagged *rec10* gene under the *Pnmt1* promoter and *Tnmt1* terminator. The recombinant plasmid ME46 was transformed into appropriate strains, confirmed by diagnostic PCRs using primers MO198, MO199, MO331 that gives a 730 bp plasmid-specific band only in the transformed strains. Further, the overexpression of Rec10 was confirmed by western blotting.

Protein expression check by immunoblotting

The expression of Rec10 from the plasmid *Pnmt1-myc-rec10* was checked by immunoblotting and cell lysates were prepared by alkaline lysis, as described previously [39]. Briefly, the strains were cultured in 10 ml NBL (-uracil) for plasmid selection and grown at 30ºC up to OD_{600} of 0.6-0.8. The washed pellets were resuspended in 150µl 1.85 M NaOH and 50µl β-mercaptoethanol (7.5%) to lyse the cells followed by 15 minutes incubation on ice. 165µl of 50% Trichloroacetic acid was added and samples were incubated for 10 minutes on ice (neutralisation step). Samples were centrifuged at 16,800xg for 10 minutes and the pellets were suspended in a 1X Laemmli buffer (6X Laemmli buffer: 375 mM Tris-HCl (pH 6.8), 35-40% glycerol, 9% SDS, 10% v/v BME, 0.015% w/v bromophenol blue) and neutralized by Tris-HCl (pH-8.0) to make the solution alkaline. Samples were boiled to elute the protein and after centrifugation at 12,000 rpm for 1 minute, the supernatant was collected and loaded on SDS-PAGE, transferred to a PVDF membrane using transfer buffer (1X Tris Glycine, 20% Methanol) for 3 hr 15 min at a constant current of 350 mA at 4ºC. The membrane was probed using 1:1000 dilutions of anti-Myc antibody (Invitrogen, MA121316) to probe for Rec10 and anti-tubulin antibody (Invitrogen, MA1-80017) to probe for tubulin as a loading control. Peroxidase AffiniPure Goat Anti-Mouse IgG (Jackson Immunoresearch, 115-035-003) was used as the secondary antibody. The blots were developed using SuperSignal West Pico PLUS Chemiluminescent Substrate (Thermo Fisher Scientific, 34580) and imaging was done using iBright CL1500 Imaging System.

Fluorescence-based tetrad assay for chromosomal segregation

The parental strains were spotted on SPA media for 2-3 days at 25ºC and meiosis was confirmed via asci formation. For imaging the tetrads, a small amount of the mating mixture was scraped off the SPA and mixed with a few drops of 50% glycerol on a glass slide and sealed off, to immobilize the cells. The cells were then visualized on a Leica DM6 upright epifluorescence microscope using Texas Red (TxR) filter to detect red (Tdtomato) fluorescence and SBL filter to detect blue (mCerulean) fluorescence. A 63X objective was used for taking images in the brightfield (BF), fluorescence and merged channels. The whole slide was scanned to capture atleast 50-200 ascii per experimental replicate. ImageJ (Fiji) software was used for processing the images and analysis was done to categorize the different classes of tetrad profiles possible as shown (Fig. 1A). The frequencies for each class of segregation profile were calculated and plotted. A minimum of 3 biological replicates were performed for each genotype and the data for individual experiments are provided in Supplementary Tables 4, 5 and 7.

Genetic recombination assay

We measured recombination across *cen3* using prototrophic/antibiotic markers (*ura4+/hygR* and *his3+)* introduced at *chk1* and near *mid1,* respectively [40]. The parental strains had two

different *ade6* mutations, *ade6-52* (showing pink colonies on YEA) and *ade6-M210/ade6-M26* (showing red colonies on YEA). Arm recombination was measured between the *mid1::his3* and *ade6* interval. This interval was referred to as the cen3-ade6 interval, since the *his3* and *ura4* markers flanking the centromere 3 are tightly linked. Other arm intervals used in this study are *ade6-arg1,* again on chromosome 3. Mating was induced between the two parental strains by spotting them on SPA media and keeping it for 2-3 days at 25°C. Post-asci formation (verified by microscopy), spores were harvested after glusulase and ethanol treatment, plated on YEA plate and incubated till colonies were formed. Individual colonies were randomly picked on supplemented YEA and after sufficient growth were replica-plated on different selectable media to measure growth in the absence of required supplements based on their genotypes. Recombination frequency was calculated as the percentage of recombinant colonies over the total number of colonies screened and the mean was plotted as bar graphs. For each genotype, the data was collected for atleast 3 independent parental colonies (biological repeats) as results of independent crosses. Error bars for all N=3 data represent SEM. The data for individual experiments are provided in Supplementary Tables 6 and 8.

Statistical Analysis

Data for the genetic recombination assays was analysed by using two-tailed Fisher's exact test. Statistical significance in different error types among the various genotypes using the fluorescence-based tetrad assay was analysed by performing the two-way ANOVA test. All the analysis was done using GraphPad Prism software.

Acknowledgements

We thank Ishan Khurma, Shruti Patil, Nandeesh Sharma, Ananya Dodamani, Purva Gupta for their technical help with yeast strain generation and genotyping. We thank MN lab members for their inputs on the manuscript and helpful discussions. We acknowledge Prof. Alexander Lorenz for sharing the spore-autonomous mCerulean and tdTomato expressing plasmids (pALo196 and pALo197) and *S. pombe* strains UoA726 and UoA727. We thank Dr. Shravan K. Mishra for the expression vector pREP4X.2 and Prof. Gerald R. Smith for sharing *S. pombe* strains. S Sen acknowledges fellowship from University Grants Commission (221610216531). This study was supported by a core grant from the Department of Biotechnology, Government of India (BT/PR44595/MED/12/953/2022) to MN and IISER Pune intramural funding. We acknowledge the IISER Pune Microscopy Facility for infrastructural support.

Disclosure and competing interest statement

Authors declare no conflict of interest

References

1. Nagaoka, S. I., Hassold, T. J. & Hunt, P. A. Human aneuploidy: mechanisms and new insights into an age-old problem. *Nat Rev Genet* **13**, 493–504 (2012).
2. Lam, I. & Keeney, S. Mechanism and Regulation of Meiotic Recombination Initiation. *Cold Spring Harb Perspect Biol* **7**, (2015).
3. Pâques, F. & Haber, J. E. Multiple pathways of recombination induced by double-strand breaks in Saccharomyces cerevisiae. *Microbiol Mol Biol Rev* **63**, 349–404 (1999).

4. Payero, L. & Alani, E. Crossover recombination between homologous chromosomes in meiosis: recent progress and remaining mysteries. *Trends Genet* (2024) doi:10.1016/J.TIG.2024.09.009.
5. Watanabe, Y. Shugoshin: Guardian spirit at the centromere. *Curr Opin Cell Biol* **17**, 590–595 (2005).
6. Clift, D. & Marston, A. L. The role of shugoshin in meiotic chromosome segregation. *Cytogenet Genome Res* **133**, 234–242 (2011).
7. Nambiar, M. & Smith, G. R. Repression of harmful meiotic recombination in centromeric regions. *Seminars in Cell and Developmental Biology* vol. 54 188–197 Preprint at https://doi.org/10.1016/j.semcdb.2016.01.042 (2016).
8. Nambiar, M., Chuang, Y. C. & Smith, G. R. Distributing meiotic crossovers for optimal fertility and evolution. *DNA Repair* vol. 81 Preprint at https://doi.org/10.1016/j.dnarep.2019.102648 (2019).
9. Nambiar, M. & Smith, G. R. Pericentromere-Specific Cohesin Complex Prevents Meiotic Pericentric DNA Double-Strand Breaks and Lethal Crossovers. *Mol Cell* **71**, 540-553.e4 (2018).
10. Lynn, A., Ashley, T. & Hassold, T. Variation in human meiotic recombination. *Annu Rev Genomics Hum Genet* **5**, 317–349 (2004).
11. Hassold, T. & Hunt, P. To err (meiotically) is human: The genesis of human aneuploidy. *Nat Rev Genet* **2**, 280–291 (2001).
12. Rockmill, B., Voelkel-Meiman, K. & Roeder, G. S. Centromere-proximal crossovers are associated with precocious separation of sister chromatids during meiosis in Saccharomyces cerevisiae. *Genetics* **174**, 1745–1754 (2006).
13. Sears, D. D., Hegemann, J. H., Shero, J. H. & Hieter, P. Cis-acting determinants affecting centromere function, sister-chromatid cohesion and reciprocal recombination during meiosis in Saccharomyces cerevisiae. *Genetics* **139**, 1159–1173 (1995).
14. Koehler, K. E. & Hassold, T. J. Human aneuploidy: lessons from achiasmate segregation in Drosophila melanogaster. *Ann Hum Genet* **62**, 467–479 (1998).
15. Koehler, K. E. *et al.* Spontaneous X chromosome MI and MII nondisjunction events in Drosophila melanogaster oocytes have different recombinational histories. *Nat Genet* **14**, 406–414 (1996).
16. Lamb, N. E. *et al.* Susceptible chiasmate configurations of chromosome 21 predispose to non-disjunction in both maternal meiosis I and meiosis II. *Nat Genet* **14**, 400–405 (1996).
17. Li, D., Roca, M., Yuecel, R. & Lorenz, A. Immediate visualization of recombination events and chromosome segregation defects in fission yeast meiosis. *Chromosoma* **128**, (2019).
18. Ottolini, C. S. *et al.* Genome-wide maps of recombination and chromosome segregation in human oocytes and embryos show selection for maternal recombination rates. *Nat Genet* **47**, 727–735 (2015).
19. Kitajima, T. S., Yokobayashi, S., Yamamoto, M. & Watanabe, Y. Distinct cohesin complexes organize meiotic chromosome domains. *Science (1979)* **300**, 1152–1155 (2003).
20. Jacobs, S. A. & Khorasanizadeh, S. Structure of HP1 chromodomain bound to a lysine 9-methylated histone H3 tail. *Science* **295**, 2080–2083 (2002).
21. Sharif, W. D., Glick, G. G., Davidson, M. K. & Wahls, W. P. Distinct functions of S. pombe Rec12 (Spo11) protein and Rec12-dependent crossover recombination (chiasmata) in meiosis I; and a requirement for Rec12 in meiosis II. *Cell Chromosome* **1**, (2002).
22. Chiang, T., Duncan, F. E., Schindler, K., Schultz, R. M. & Lampson, M. A. Evidence that weakened centromere cohesion is a leading cause of age-related aneuploidy in oocytes. *Curr Biol* **20**, 1522 (2010).
23. Kitajima, T. S. *et al.* Shugoshin collaborates with protein phosphatase 2A to protect cohesin. *Nature* **441**, 46–52 (2006).

24. Nonaka, N. *et al.* Recruitment of cohesin to heterochromatic regions by Swi6/HP1 in fission yeast. *Nat Cell Biol* **4**, 89–93 (2002).
25. Motamedi, M. R. *et al.* HP1 proteins form distinct complexes and mediate heterochromatic gene silencing by nonoverlapping mechanisms. *Mol Cell* **32**, 778–790 (2008).
26. Marston, A. L. Shugoshins: Tension-Sensitive Pericentromeric Adaptors Safeguarding Chromosome Segregation. *Mol Cell Biol* **35**, 634–648 (2015).
27. Hunter, N. Meiotic Recombination: The Essence of Heredity. *Cold Spring Harb Perspect Biol* **7**, a016618 (2015).
28. Vincenten, N. *et al.* The kinetochore prevents centromere-proximal crossover recombination during meiosis. *Elife* **4**, (2015).
29. Kuhl, L. M. & Vader, G. Kinetochores, cohesin, and DNA breaks: Controlling meiotic recombination within pericentromeres. *Yeast* **36**, 121–127 (2019).
30. Gruhn, J. R. *et al.* Chromosome errors in human eggs shape natural fertility over reproductive life span. *Science (1979)* **365**, 1466–1469 (2019).
31. Fowler, K. R., Gutiérrez-Velasco, S., Martín-Castellanos, C. & Smith, G. R. Protein Determinants of Meiotic DNA Break Hot Spots. *Mol Cell* **49**, 983–996 (2013).
32. Yamamoto, A. & Hiraoka, Y. Monopolar spindle attachment of sister chromatids is ensured by two distinct mechanisms at the first meiotic division in fission yeast. *EMBO J* **22**, 2284 (2003).
33. Riedel, C. G. *et al.* Protein phosphatase 2A protects centromeric sister chromatid cohesion during meiosis I. *Nature* **441**, 53–61 (2006).
34. Garcia-Cruz, R. *et al.* Dynamics of cohesin proteins REC8, STAG3, SMC1 beta and SMC3 are consistent with a role in sister chromatid cohesion during meiosis in human oocytes. *Hum Reprod* **25**, 2316–2327 (2010).
35. Kitajima, T. S., Miyazaki, Y., Yamamoto, M. & Watanabe, Y. Rec8 cleavage by separase is required for meiotic nuclear divisions in fission yeast. *EMBO Journal* **22**, 5643–5653 (2003).
36. Mihalas, B. P. *et al.* Age-dependent loss of cohesion protection in human oocytes. *Curr Biol* **34**, 117-131.e5 (2024).
37. Smith, G. R. Genetic analysis of meiotic recombination in Schizosaccharomyces pombe. *Methods in Molecular Biology* **557**, 65–76 (2009).
38. Gietz, R. D. & Woods, R. A. Transformation of yeast by lithium acetate/single-stranded carrier DNA/polyethylene glycol method. *Methods Enzymol* **350**, 87–96 (2002).
39. Knop M *et al.* Epitope tagging of yeast genes using a PCR-based strategy: more tags and improved practical routines - PubMed. *Yeast* **15**, 963–972 (1999).
40. Ellermeier, C. *et al.* RNAi and heterochromatin repress centromeric meiotic recombination. *Proc Natl Acad Sci U S A* **107**, 8701–8705 (2010).

Figure Legends

Figure 1. Elevated pericentric crossovers lead to increased meiosis I segregation defects. A. Schematic representation of the fluorescence-based tetrad assay for segregation fidelity. Representative images of each type of segregation error are shown. The mirror patterns of fluorophore inheritance in each error type are not shown. **B.** Plot showing frequency of normal, centromeric crossover (C-CO) or reverse segregation (RS), meiosis I (MI) and meiosis II (MII) segregation errors in *rec10Δ* and *rec10Δ rec10ee* (ectopically expressed) genotypes. **C.** Plot showing frequency of normal, centromeric crossover (C-CO) or reverse segregation (RS), meiosis I (MI) and meiosis II (MII) segregation errors in wild type, *rec10ee, rec10-CD rec10ee, rec10(mut)-CD rec10ee* and *rec10-CD(mut)* genotypes. **D.** Bar

graph showing distribution of MI non-disjunction (NDJ) and MI premature separation of sister chromatids (PSSC) events among the total MI errors in *rec10Δ rec10ee, rec10-CD rec10ee, rec10(mut)-CD rec10ee* and *rec10-CD(mut)* genotypes. All data are mean ± SEM (n = 3 experiments), assaying 509, 477, 890, 367, 479, 517 and 560 tetrads for *rec10Δ, rec10Δ rec10ee,* wild type, *rec10ee, rec10-CD rec10ee, rec10(mut)-CD rec10ee* and *rec10-CD(mut)*, respectively. ****p <0.0001 (two-way ANOVA test); ***p <0.001; **p <0.01; ns p >0.05. The data for individual experiments are provided in Supplementary Table 4.

Figure 2. Abolishing chromosomal arm crossovers lead to elevated defects during meiosis I. A. Plot showing frequency of normal, centromeric crossover (C-CO) or reverse segregation (RS), meiosis I (MI) and meiosis II (MII) segregation errors in wild type, *rec10Δ, rec12Δ, rec11Δ* and phosphomutant *rec11(5A)* genotypes. **B.** Bar graph showing distribution of MI non-disjunction (NDJ) and MI premature separation of sister chromatids (PSSC) events among the total MI errors in wild type, *rec10Δ, rec12Δ, rec11Δ* and *rec11(5A)* genotypes. All data are mean ± SEM (n = 3 experiments), assaying 834, 509, 333, 489 and 364 tetrads for wild type, *rec10Δ, rec12Δ, rec11Δ* and *rec11(5A)*, respectively. ****p <0.0001 (two-way ANOVA test); ***p <0.001; ns p >0.05. **C.** Recombinant frequency (RF) across *ade6-arg1* arm interval in *wild type, rec11ee, rec11Δ, rec11Δ rec11ee* (ectopically expressed), *rec11(5A),* and *rec11(5A) rec11e*e genotypes. Data are mean ± SEM (n = 3 experiments), assaying 390, 389, 469, 294, 672 and 411 spore colonies for *wild type, rec11ee, rec11Δ, rec11Δ rec11ee*, *rec11(5A),* and *rec11(5A) rec11e*e, respectively. ****p < 0.0001 (two-tailed Fisher's exact test); ns p >0.05. The data for individual experiments are provided in Supplementary Tables 4, 5 and 6.

Figure 3. Loss of centromeric cohesion and heterochromatin result in meiosis II errors. A. Schematic representation of the different types of mutants used to disrupt the centromeric cohesion and the pericentric heterochromatin. **B.** Plot showing frequency of normal, centromeric crossover (C-CO) or reverse segregation (RS), meiosis I (MI) and meiosis II (MII) segregation errors in wild type, *psc3Δ, swi6Δ, sgo1Δ, ppa2Δ* and *chp2Δ* genotypes. Data are mean ± SEM (n = 3 experiments), assaying 832, 364, 377, 415, 443 and 615 tetrads for wild type, *psc3Δ, swi6Δ, sgo1Δ, ppa2Δ* and *chp2Δ*, respectively. ****p <0.0001 (two-way ANOVA test); ***p <0.001; ns p >0.05. **C-D.** Recombinant frequency (RF) across *cen3-ade6* arm interval **(C)** and *cen3* **(D)** in wild type, *sgo1Δ* and *ppa2Δ* genotypes. Data are mean ± SEM (n = 3 experiments), assaying 374, 683 and 576 spore colonies for wild type, *sgo1Δ* and *ppa2Δ*, respectively. *p <0.05 (two-tailed Fisher's exact test); ns p >0.05. The data for individual experiments are provided in Supplementary Tables 7 and 8.

Figure 4. Reduced centromeric cohesion alters the subtype of meiosis I errors in the presence of increased centromeric crossovers. A. Bar graph showing distribution of MI non-disjunction (NDJ) and MI premature separation of sister chromatids (PSSC) events among the total MI errors in *psc3+ rec8-CD rec11-CD rec11ee* (ectopically expressed), *psc3Δ rec8ee rec11ee*, *psc3Δ rec8-CD rec11-CD rec11ee* and *psc3Δ rec8-CD rec11(5A)-CD rec11ee* genotypes. All data are mean ± SEM (n = 3 experiments), assaying 408, 364, 477 and 647 tetrads for *psc3+ rec8-CD rec11-CD rec11ee*, *psc3Δ rec8ee rec11ee*, *psc3Δ rec8-CD rec11-CD rec11ee* and *psc3Δ rec8-CD rec11(5A)-CD rec11ee*, respectively. For the other error types, refer Supplementary Figure 2C legend. In all these genotypes, *rec8-CD* allele is ectopically expressed. **B.** Plot showing frequency of normal, centromeric crossover (C-CO) or reverse segregation (RS), meiosis I (MI) and meiosis II (MII) segregation errors in *rec10-CD rec10ee,* r*ec10-CD rec10ee swi6Δ* and *swi6Δ* genotypes. **C.** Bar graph showing distribution of MI non-disjunction (NDJ) and MI premature separation of sister chromatids (PSSC) events among the total MI errors in *rec10-CD rec10ee* and r*ec10-CD rec10ee swi6Δ* genotypes. All data are mean ± SEM (n = 3 experiments), assaying 479, 713 and 377 tetrads for *rec10-CD rec10ee,* r*ec10-CD rec10ee swi6Δ* and *swi6Δ,* respectively. ****p <0.0001 (two-way ANOVA test); ***p <0.001; **p <0.01; *p <0.05; ns p >0.05. The data for individual experiments are provided in Supplementary Tables 4 and 7.

Figure 5. Model to explain the elevated levels of MI errors upon elevated centromeric crossovers. Proteolytic cleavage of cohesins in the chromosomal arms results in resolution of chiasma during anaphase I. In contrast, the population of “protected” centromeric cohesins may hinder the proper and timely resolution of centromeric crossovers resulting in homologs being stuck or entangled with each other, unable to separate, thereby resulting in increased nondisjunction events at meiosis I. At the same time, defects in monopolar attachment of the kinetochores at MI, may result elevated propensity for premature separation of sister chromatids (PSSC), thereby contributing significantly to the MI errors due to presence of centromere-proximal crossovers during meiosis.

Figure 1

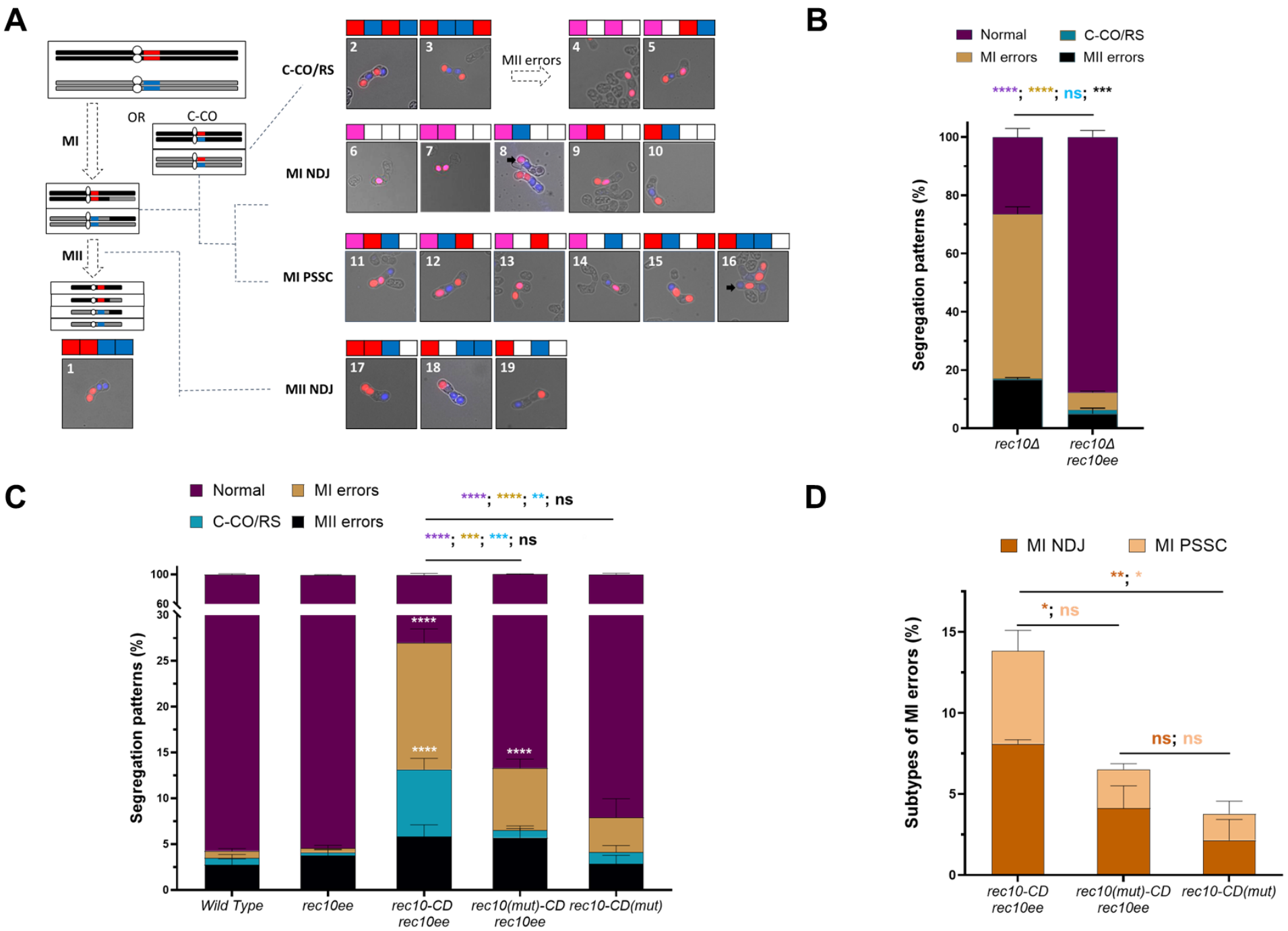
A
OR
C-CO
MI
MII
C-CO/RS
MI NDJ
MI PSSC
MII NDJ
MII errors
B
Normal
C-CO/RS
MI errors
MII errors
****; ****; ns; ***
Segregation patterns (%)
rec10Δ
rec10Δ rec10ee
C
Normal
MI errors
C-CO/RS
MII errors
****; ****; **; ns
****; ***; ***; ns
Segregation patterns (%)
Wild Type
rec10ee
rec10-CD rec10ee
rec10(mut)-CD rec10ee
rec10-CD(mut)
D
MI NDJ
MI PSSC
**; *
*; ns
ns; ns
Subtypes of MI errors (%)
rec10-CD rec10ee
rec10(mut)-CD rec10ee
rec10-CD(mut)

Figure 2

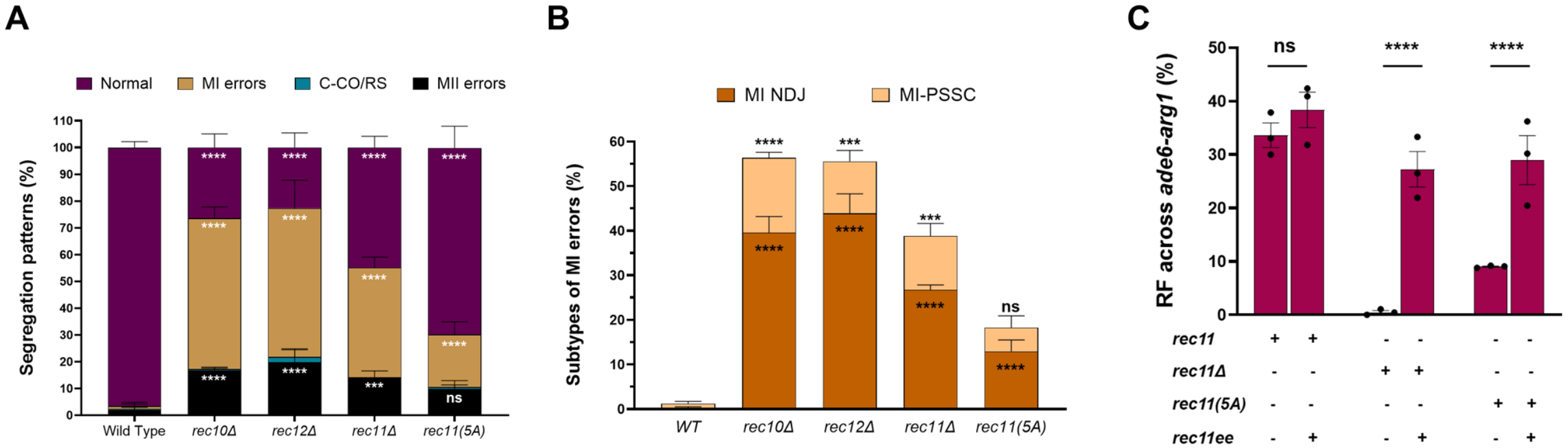
A
Normal
MI errors
C-CO/RS
MII errors
Segregation patterns (%)
Wild Type
rec10Δ
rec12Δ
rec11Δ
rec11(5A)
B
MI NDJ
MI-PSSC
Subtypes of MI errors (%)
WT
rec10Δ
rec12Δ
rec11Δ
rec11(5A)
C
RF across ade6-arg1 (%)
rec11
rec11Δ
rec11(5A)
rec11ee

Figure 3

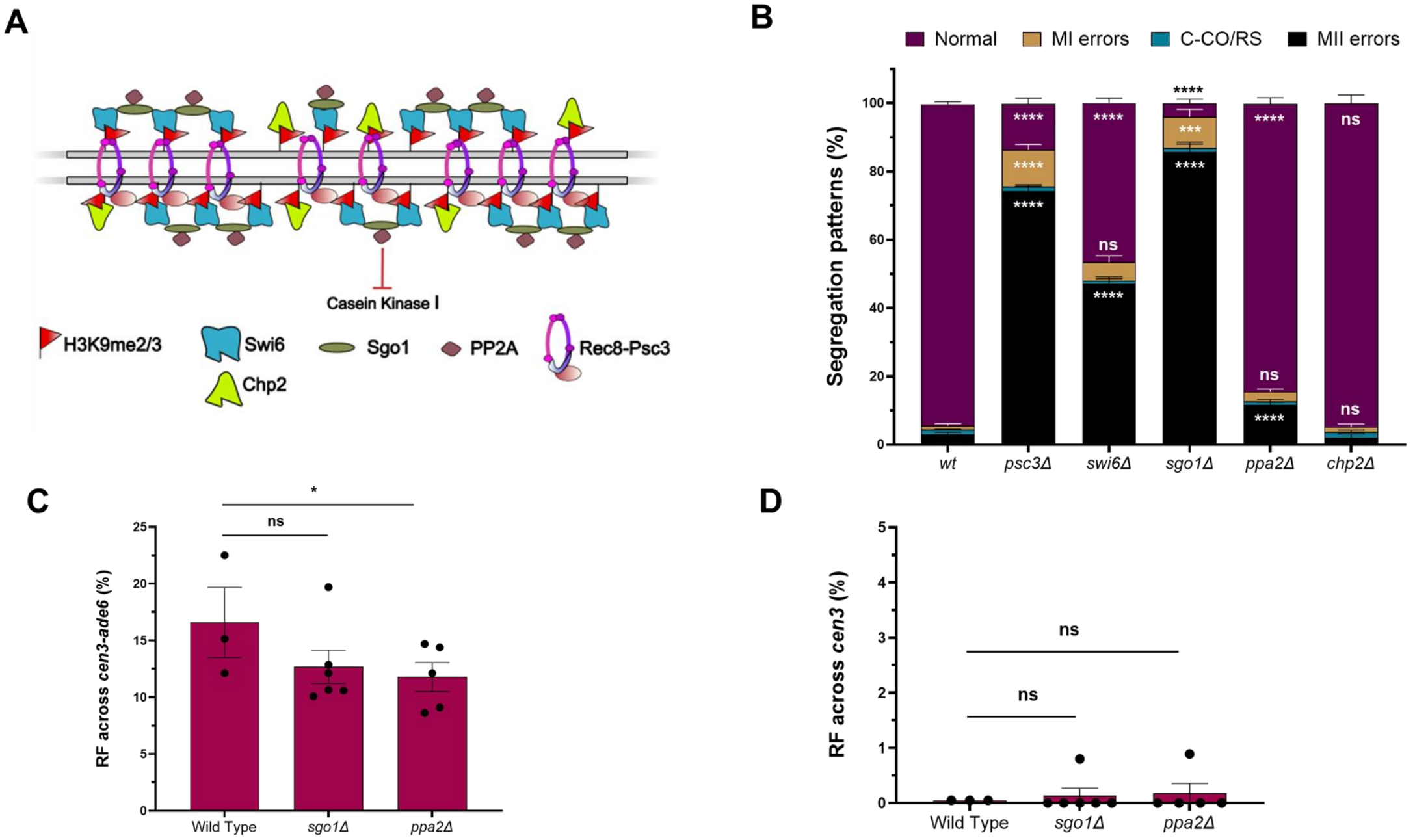
A
Casein Kinase I
H3K9me2/3
Swi6
Sgo1
PP2A
Rec8-Psc3
Chp2
B
Normal
MI errors
C-CO/RS
MII errors
Segregation patterns (%)
wt
psc3Δ
swi6Δ
sgo1Δ
ppa2Δ
chp2Δ
C
RF across cen3-ade6 (%)
Wild Type
sgo1Δ
ppa2Δ
D
RF across cen3 (%)
Wild Type
sgo1Δ
ppa2Δ

Figure 4

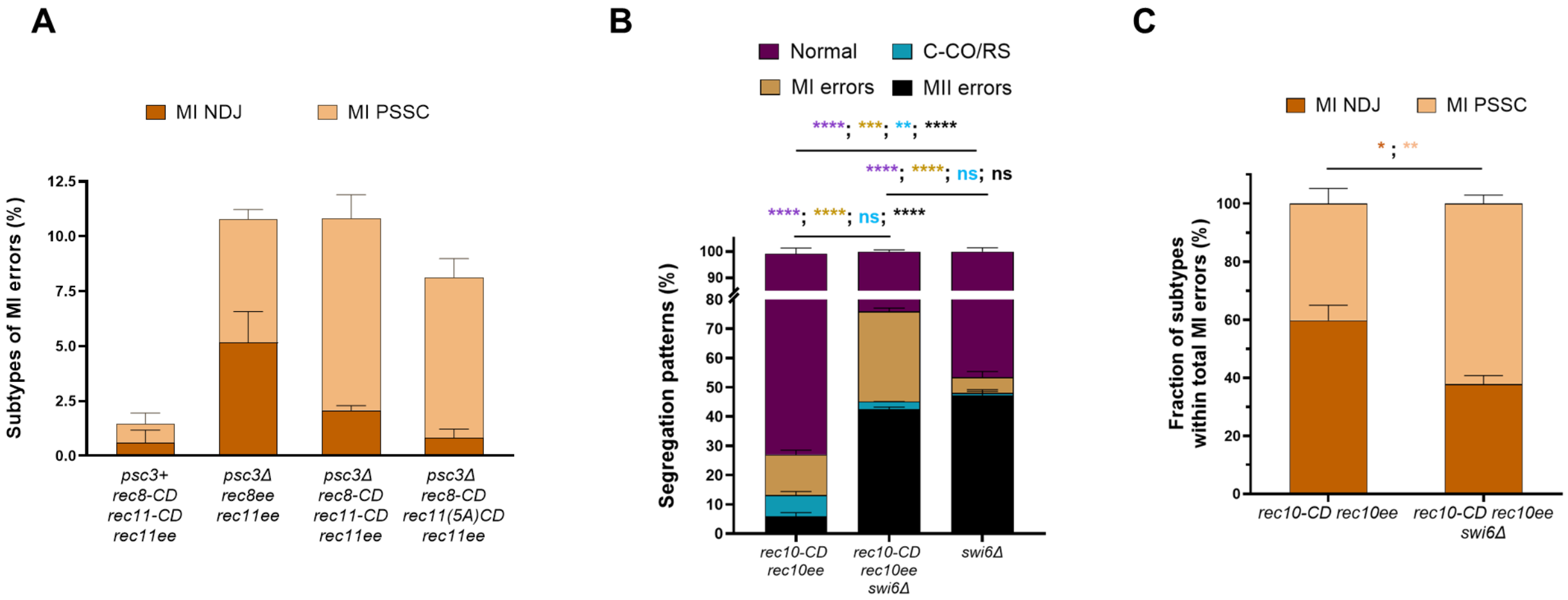
A
MI NDJ
MI PSSC
Subtypes of MI errors (%)
12.5
10.0
7.5
5.0
2.5
0.0
psc3+ rec8-CD rec11-CD rec11ee
psc3Δ rec8ee rec11ee
psc3Δ rec8-CD rec11-CD rec11ee
psc3Δ rec8-CD rec11(5A)CD rec11ee
B
Normal
C-CO/RS
MI errors
MII errors
****; ***; **; ****
****; ****; ns; ns
****; ****; ns; ****
Segregation patterns (%)
100
90
80
70
60
50
40
30
20
10
0
rec10-CD rec10ee
rec10-CD rec10ee swi6Δ
swi6Δ
C
MI NDJ
MI PSSC
* ; **
Fraction of subtypes within total MI errors (%)
100
80
60
40
20
0
rec10-CD rec10ee
rec10-CD rec10ee swi6Δ

Figure 5

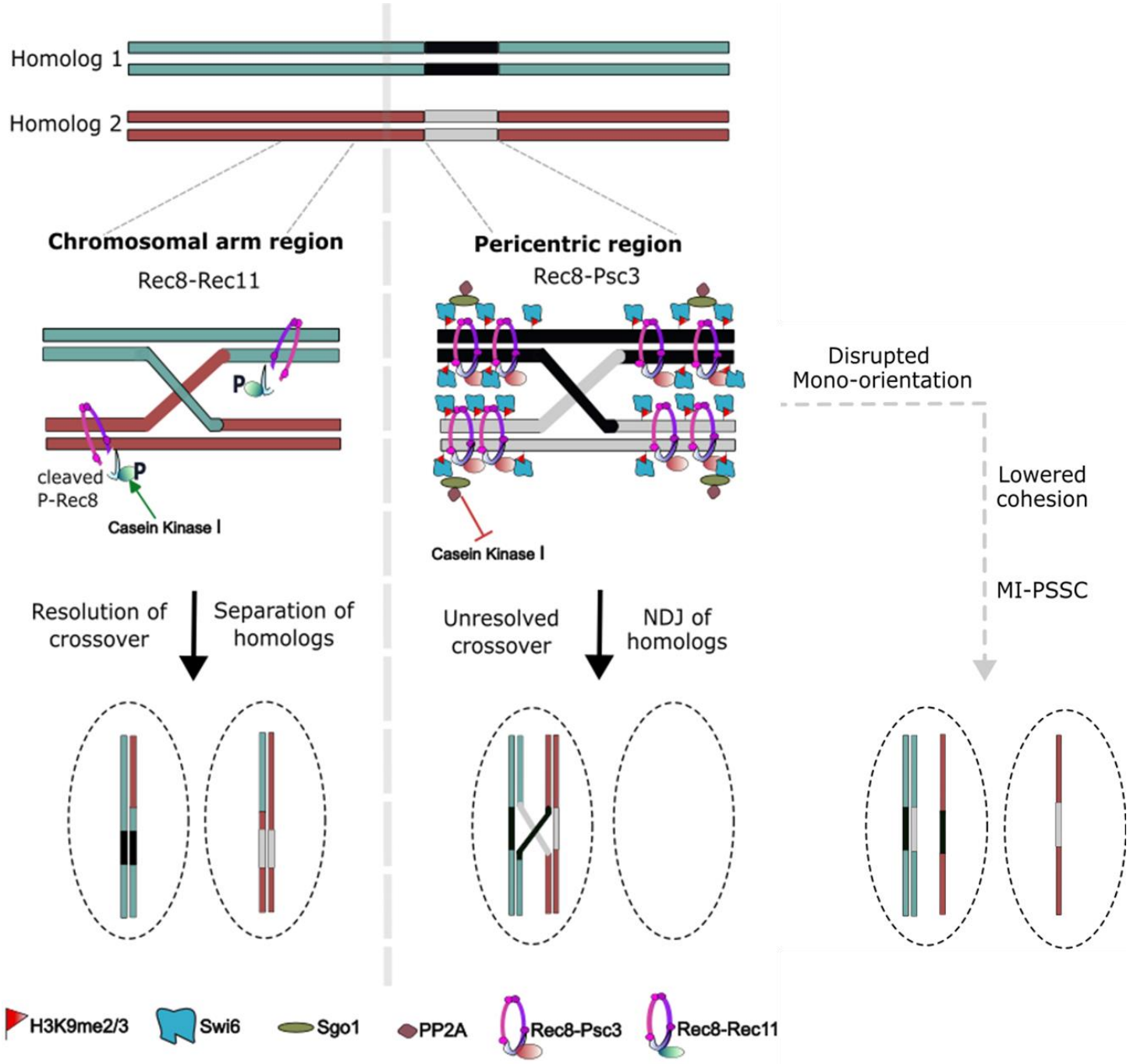
Homolog 1
Homolog 2
Chromosomal arm region
Rec8-Rec11
P
cleaved
P-Rec8
P
Casein Kinase I
Pericentric region
Rec8-Psc3
Casein Kinase I
Disrupted
Mono-orientation
Lowered
cohesion
MI-PSSC
Resolution of
crossover
Separation of
homologs
Unresolved
crossover
NDJ of
homologs
H3K9me2/3
Swi6
Sgo1
PP2A
Rec8-Psc3
Rec8-Rec11